Chemical Science

ROYAL SOCIETY OF CHEMISTRY

EDGE ARTICLE

View Article Online
View Journal | View Issue



Cite this: *Chem. Sci.*, 2023, **14**, 5956

All publication charges for this article have been paid for by the Royal Society of Chemistry

# Photochemically controlled activation of STING by CAIX-targeting photocaged agonists to suppress tumor cell growth†

Chunyong Ding, ‡*[ag] Mengyan Du,‡[bef] Zhi Xiong,‡[ad] Xue Wang,‡[a] Hongji Li,[a] Ende He,[a] Han Li,[bf] Yijing Dang, [c] Qing Lu,[a] Shicong Li,[a] Ruoxuan Xiao,[a] Zhiai Xu, [c] Lili Jing,*[a] Liufu Deng,[a] Xiyuan Wang, [b] Meiyu Geng,[be] Zuoquan Xie*[be] and Ao Zhang*[a]

Controllable activation of the innate immune adapter protein – stimulator of interferon genes (STING) pathway is a critical challenge for the clinical development of STING agonists due to the potential "on-target off-tumor" toxicity caused by systematic activation of STING. Herein, we designed and synthesized a photo-caged STING agonist **2** with a tumor cell-targeting carbonic anhydrase inhibitor warhead, which could be readily uncaged by blue light to release the active STING agonist leading to remarkable activation of STING signaling. Furthermore, compound **2** was found to preferentially target tumor cells, stimulate the STING signaling in zebrafish embryo upon photo-uncaging and to induce proliferation of macrophages and upregulation of the mRNA expression of STING as well as its downstream NF-kB and cytokines, thus leading to significant suppression of tumor cell growth in a photo-dependent manner with reduced systemic toxicity. This photo-caged agonist not only provides a powerful tool to precisely trigger STING signalling, but also represents a novel controllable STING activation strategy for safer cancer immunotherapy.

Received 12th April 2023
Accepted 5th May 2023

DOI: 10.1039/d3sc01896b

rsc.li/chemical-science



## Introduction

The stimulator of interferon genes (STING) is a major component of the innate immune system that senses cytosolic double stranded DNA (dsDNA) and triggers antiviral and anti-tumour immunity.[1–3] STING is an endoplasmic reticulum-transmembrane adaptor protein for recognition of 2′,3′-cyclic guanosine monophosphate–adenosine monophosphate (cGAMP), which is a second messenger produced by dsDNA recognition receptor cyclic guanosine monophosphate–adenosine monophosphate synthase (cGAS).[4–9] Upon binding with cGAMP, STING undergoes a large conformational change to trigger a series of downstream signalling activation events, leading to production of type I interferons and many other inflammatory cytokines,[10–12] which can induce cross-priming of tumor-specific antigens and facilitate a T cell-inflamed tumor microenvironment, and eventually promote the adaptive immune response for antitumor immunity.[13–15] Therefore, STING is a promising tumour immunotherapeutic target for turning immunologically "cold" tumor to "hot".[16–18] STING agonists with various chemotypes have been extensively explored.[19–26] For instance, small molecule MSA-2 with the benzothiophene scaffold was revealed to be an orally available STING agonist showing potent systemic antitumor immunity with promising clinical potential.[26] However, activation of STING is a double-edged sword when manipulated as cancer immunotherapy. Due to the ubiquitous expression of STING in both tumor and normal tissues, systemic administration of STING agonists can result in "on-target off-tumor" toxicity, such as an uncontrolled cytokine storm and autoimmunity.[13,27] Over-activation of STING results in persistent generation of cytokines, not only creating an inflammatory tumor microenvironment (TME) to promote tumour development, but also inducing cell stress and death in T-lymphocytes.[28,29]

[a]*Shanghai Frontiers Science Center of Drug Target Identification and Delivery, College of Pharmaceutical Sciences, National Key Laboratory of Innovative Immunotherapy, Shanghai Jiao Tong University, Shanghai 200240, China. E-mail: chunding@sjtu.edu.cn; lilijing@sjtu.edu.cn; ao6919zhang@sjtu.edu.cn; Tel: +86 21 50806035*

[b]*State Key Laboratory of Drug Research, Shanghai Institute of Materia Medica (SIMM), Chinese Academy of Sciences, Shanghai 201203, China. E-mail: zqxie@simm.ac.cn*

[c]*School of Chemistry and Molecular Engineering, East China Normal University, Shanghai 200241, China*

[d]*School of Pharmacy, Nanchang University, Jiangxi 330000, China*

[e]*University of Chinese Academy of Sciences, Beijing, 100049, China*

[f]*School of Life Science and Technology, ShanghaiTech University, Shanghai, 200031, China*

[g]*Zhangjiang Institute of Advanced Study, Shanghai Jiao Tong University, Shanghai 200240, China*

† Electronic supplementary information (ESI) available: Details of the experimental procedure, spectroscopic data and copies of the $^{1}H$ and $^{13}C$ NMR spectra of the products. See DOI: https://doi.org/10.1039/d3sc01896b

‡ These authors contributed equally to this work.

Although intratumoral delivery of STING agonists has the potential to avoid the off-tumor side effects, this strategy suffers from limited application to a narrow subset of tumors.[13,22] Accordingly, controllable activation of STING in cancerous tissue is critical for STING agonists as a new stimulatory immuno-oncology therapy.

Due to the non-invasive properties and spatiotemporal accuracy, the utilization of light to precisely regulate biological processes has become increasingly evident.[30–32] Particularly, the photo-induced drug release strategy has received considerable attention in medicinal research owing to the controllable bioactivity in the desired tissues and cells while avoiding side effects elsewhere.[33,34] Similar to a prodrug strategy, a photo-removable protecting group (PPG) is utilized to mask the key pharmacophore of a drug (warhead).[35] The resulting photo-caged drug is then uncaged by irradiation with light of an appropriate wavelength to liberate the bioactive parent molecule, thereby exhibiting desired therapeutic effects with low systemic side effects.[36,37] Therefore, it would be of critical importance to add a photo-controllable trigger on a potent STING agonist,[37b] thus enabling its spatial activation in desirable tissues and cells to facilitate precise controllable activation of cellular STING as well as to eliminate potential off-tumor toxicity.

Herein, we describe the design, synthesis, and biological evaluation of photo-activatable STING agonists **1** and **2** based on MSA-2. The principle of photo-triggered activation of STING signalling is depicted in Fig. 1. The caged agonists with or without a tumor-specific carbonic anhydrase warhead in the absence of light irradiation are unable to stimulate STING, whereas upon light irradiation, the active agonist MSA-2 is irreversibly released, leading to STING activation and secretion of interferon-stimulated genes (ISGs). This photoactivatable strategy may offer a promising option to precisely manipulate the STING signalling and eliminate systemic side effects caused by the STING agonist.

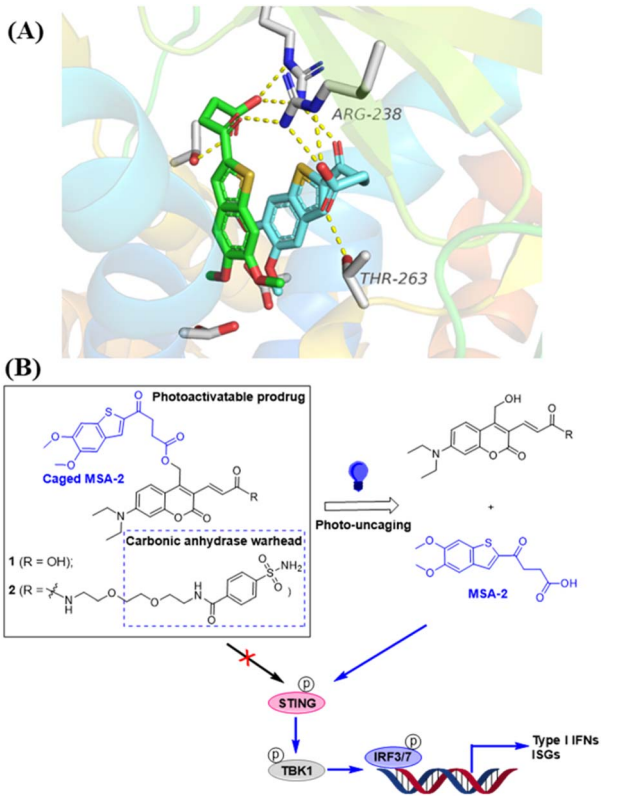


Fig. 1 Design of photo-activatable STING agonists. (A) Co-crystal structure analysis of MSA-2 bound to human STING protein (PDB: 6UKM26) identifies the terminal oxobutanoic acid as the critical structural motif for the activation of STING, evidenced by several key hydrogen bond interactions (orange dashed line). (B) STING agonist MSA-2 is caged with DEACM PPGs placed at the terminal oxobutanoic acid, which prevents the activation of the STING signalling. Irradiation with blue light at 450 nm removes the caging group to release MSA-2, which activates STING to induce the phosphorylation of the downstream signalling.

## Results and discussion

### Design of photoactivatable STING agonists

The photocaged STING agonist was designed on the basis of the benzothiophene oxobutanoic acid scaffold of MSA-2, which is an orally available non-nucleotide STING agonist recently disclosed by Merck.[26] According to the X-ray crystal structure of MSA-2 bound to human STING (Fig. 1A), the carboxylate group not only forms a hydrogen bond with the proximal Thr263, but also forms hydrogen bonds (yellow dashed lines) with the Arg238 guanidinium group side chain across the STING homodimer. These interactions are critical and responsible for STING activation.[26] Due to the high quantum yield and aqueous solubility of the 7-(diethylamino)-4-(hydroxymethyl)coumarin (DEACM),[38,39] we used it as the PPG to cage the carboxylate group of MSA-2 to yield compound **1**, in which the carboxylic H-bonding interactions of MSA-2 were masked to turn "OFF" its STING activity (Fig. 1B). Due to the photoactive cleaving nature of DEACM, **1** can be easily uncaged under 450 nm blue light to recover MSA-2 to turn "ON" its STING signalling. To increase tumor tissue-specific targeting, a carbonic anhydrase IX (CAIX) ligand (arylsulfonamide) is attached to the acrylic acid moiety of the DEACM component of **1**, leading to a CAIX-targeting photoactivatable STING agonist **2** (Fig. 1B). Since CAIX is generally over-expressed in various aggressive tumors over normal tissues,[40,41] this targeted photoactivatable molecule **2** represents a photo-controllable STING agonist specifically targeting cancer.

### Chemical synthesis of photo-caged STING agonists

As described in Scheme 1, the synthesis of **1** was commenced from the fully protected coumarin **4**, which was readily prepared from 7-amino-4-methyl coumarin **3** by following a five-step literature procedure.[39] Selective removal of the silyl group in **4** with tetrabutylammonium fluoride (TBAF) afforded alcohol coumarin **6**, which was further coupled with MSA-2 in the presence of EDCI/HOBT followed by deprotection of the *tert*-butyl group under TFA to give the desired product **1**. Deprotection of the *tert*-butyl group in **6** with TFA afforded the

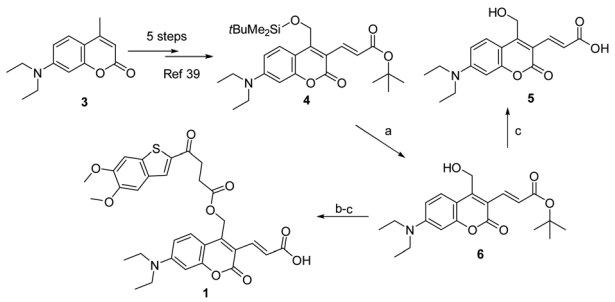


Scheme 1 Synthesis of the photocaged sting agonist **1**. Reagents and conditions: (a) TBAF, THF, DCM, rt, 1 h, 70%; (b) MSA-2, EDCI, HOBT, DIPA, rt, overnight, 69%; (c) TFA, DCM, rt, 1 h, 90%.

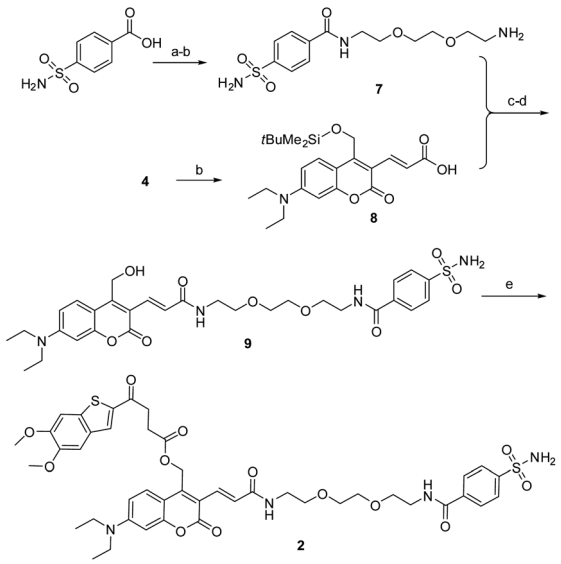


Scheme 2 Synthesis of the CAIX-targeting photoactivatable sting agonist **2**. Reagents and conditions: (a) *tert*-butyl (2-(2-(2-aminoethoxy)ethoxy)ethyl)carbamate, EDCI, HOBT, DIPA, rt, overnight, 70%; (b) TFA, DCM, rt, 1 h; (c) EDCI, HOBT, DIPA, rt, overnight, 78%; (d) TBAF, THF, rt, 1 h, 68%; (e) MSA-2, EDCI, HOBT, DIPA, rt, overnight, 69%.

carboxylic acid coumarin **5** as the photo-releasing side product of **1**. The synthesis of **2** is described in Scheme 2. 4-Sulfamoylbenzoic acid was amidized with *tert*-butyl(2-(2-(2-aminoethoxy)ethoxy)ethyl)carbamate followed by Boc-deprotection to give linker **7**. Selective deprotection of the *tert*-butyl group in **4** with TFA provided carboxylic acid **8**, which was further coupled with **7** followed by deprotection of the silyl group to give alcohol coumarin **9**. Esterization of **9** with MSA-2 using EDCI/HOBT furnished the desired product **2**.

## Photochemical properties of photo-caged STING agonists 1 and 2

The photochemical properties of the caged STING agonists **1** and **2** were investigated under physiological conditions. The absorbance and fluorescence spectra were investigated in PBS buffer (10 mM, pH = 7.4, containing 5% DMSO, v/v). As shown in Fig. S1A,† compound **1** displayed two absorbance peaks centred at 325 and 450 nm, respectively, representing the maximum absorption wavelength of MSA-2 and compound **5**. Upon excitation at 450 nm, obvious fluorescence emission peaking at 525 nm was observed for **1** (Fig. S1B†). Similar photochemical behaviours were also observed in the case of **2** (Fig. S1C and D†). The photo-release of MSA-2 from the caged agonists **1** and **2**, respectively, were investigated by high-performance liquid chromatography (HPLC). Under irradiation with 450 nm blue light, the caging groups were readily removed, and the peaks of **1** and **2** decreased gradually along with the accumulation of MSA-2 and PPGs **5** and **9**, as well as an unknown side product (Fig. 2). The high efficiency of photo-cleavage of **2** allowed for nearly complete degradation within 40 min of irradiation (Fig. 2B). Moreover, no significant spontaneous hydrolysis of **2** in PBS buffer (Fig. S2†) and human plasma (Fig. S3†) at 37 °C was observed in the HPLC-MS assay, indicating its good stability in buffer (>95% remaining at 24 h) and plasma (>80% remaining at 5 h). Therefore, the caged **2** is suitable for various physiological assays within a short time of irradiation by biocompatible visible (450 nm) light.

## Compounds 1 and 2 photo-controllably activate STING downstream ISG signalling

THP1-Dual cells, which possess the STING downstream ISGs reporter, were used to evaluate the photo-activation effects of the caged agonists **1** and **2** on the STING signalling. Compounds

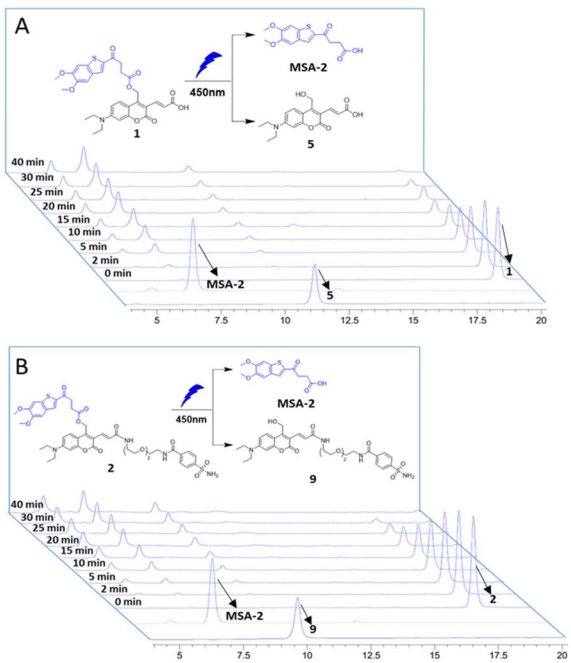


Fig. 2 Photouncaging of compounds **1** and **2** (0.5 mM) in $CH_3CN$/PBS buffer. HPLC analysis of compounds **1** (A) and **2** (B) uncaging with 450 nm blue light (intensity: 6.7 nm W $cm^{-2}$), exhibiting efficient photochemical conversion to the desired MSA-2 in a time-dependent manner. Samples with light irradiation for different times are stacked. The peaks of compounds MSA-2, **1**, **2**, **5** and **9** are labelled with arrows.

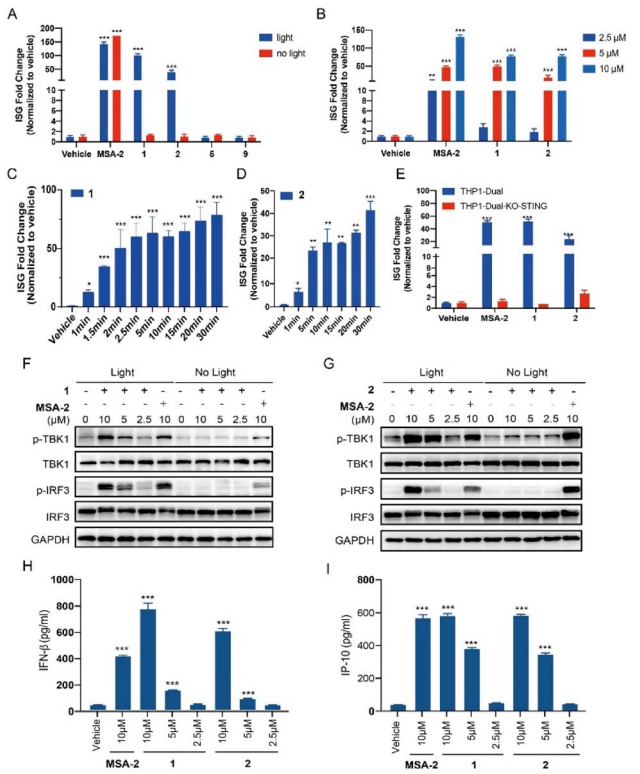


Fig. 3 Photo-controllable activation on the STING downstream signalling pathway under blue light. (A) THP1-Dual cells were treated with each compound (MSA-2, **1**, **2**, **5**, and **9**) at 10 μM or vehicle (0.1% DMSO), in the presence or absence of blue light (450 nm) for 15 min and then incubated for 24 h. (B) Dose-dependent activation on the ISG reporter of compounds **1** and **2** in THP1-Dual cells under blue light irradiation for 15 min followed by incubation for 24 h. (C) Time-dependent activation on the ISG reporter of compound **1** (5 μM) in THP1-Dual cells under blue light (40 mA, 3.35 mW $cm^{-2}$) for indicated times, followed by incubation for 24 h. (D) Time-dependent activation on the ISG reporter of compound **2** (5 μM) in THP1-Dual cells under blue light (80 mA, 6.7 mW $cm^{-2}$) for indicated times, followed by incubation for 24 h. (E) Activation of compounds **1** and **2** (5 μM) on the ISG reporter was dependent on STING under light irradiation for 15 min. The ISG fold change was calculated relative to the vehicle control, and the tests were carried out in triplicate. (F and G) THP1-Dual cells were treated with the indicated concentration of compounds (MSA-2, **1** and **2**) with or without 15 min blue light exposure, and then incubated for 4 h. The expression of proteins was determined by western blotting. (H) IFN-β secretion of THP1-Dual cells upon treatment with compounds (MSA-2, **1** and **2**) for 24 h after 15 min of blue light exposure. (I) IP-10 secretion of THP1-Dual cells upon treatment with compounds (MSA-2, **1** and **2**) for 24 h after 15 min of blue light exposure. Results are expressed as mean ± SEM from two independent experiments. *$p$ < 0.05, **$p$ < 0.01, ***$p$ < 0.001, as compared to the vehicle using one-way ANOVA.

**1** and **2** were tested on the induction of ISG reporter in the presence or absence of blue light (450 nm) irradiation. As depicted in Fig. 3A, MSA-2 as the positive control significantly stimulated the ISG reporter, which was independent of the irradiation of blue light. Neither **1** nor **2** at 10 μM induced any ISG reporter responses without light irradiation, which validated our hypothesis that caging the carboxylic acid moiety of MSA-2 nearly abolished STING activity. Upon being irradiated with 450 nm blue light, both compounds dramatically activated the ISG reporter with approximately 50- and 100-fold increment, respectively, which is comparable to that of MSA-2. No activation was observed for PPGs **5** and **9** under the same irradiation conditions. Moreover, both **1** and **2** dose-dependently activated the ISG signalling in THP1-Dual cells under 15 min irradiation of blue light (Fig. 3B), as well as time-dependently activating the ISG signalling in THP1-Dual cells under irradiation of blue light (Fig. 3C and D). These results suggest that both **1** and **2** could photo-controllably activate STING signalling with the potential of spatiotemporal accuracy. To determine if the photo-induced activation of the ISG reporter is dependent on STING protein, we further investigated the photo-induced effects of **1** and **2** in THP1-Dual KO-STING cells. As shown in Fig. 3E, both **1** and **2** were active in the wild type cells, but totally lost their photo-induced STING activity in THP1-Dual KO-STING cells, indicating the photoactivatable agonists **1** and **2** exerted their effects through targeting STING.

## Both 1 and 2 induce phosphorylation of STING downstream signalling and secretion of IFN-β and IP-10 in a light-dependent manner

We also examined the photo-triggered effects of **1** and **2** on the downstream TBK1/IRF3 phosphorylation and cytokines secretion at 2.5 μM, 5 μM, and 10 μM, respectively. As expected, both **1** and **2** failed to induce the phosphorylation of the TBK1 and IRF3 in the absence of blue light exposure (Fig. 3F and G). However, after a period of 15 min of light irradiation, the phosphorylation of STING downstream signalling was significantly increased in a dose-dependent manner (Fig. 3F and G). As a contrast, MSA-2 significantly phosphorylated TBK1 and IRF3, which was independent of irradiation. The photo-induced secretion of IFN-β and IP-10 in THP1-Dual cells, two critical cytokines of the ISG signalling pathway, was further determined in an ELISA assay. As shown in Fig. 3H and I, both **1** and **2** dose-dependently increased the secretion of IFN-β and IP-10 under 15 min light irradiation at concentrations ranging from 2.5 to 10 μM. Both **1** and **2** can activate the STING downstream signalling pathway in a photo-controllable manner.

## Compound 2 binds to CAIX on the membrane of tumor cells

CAIX is highly over-expressed on the membrane of various cancer cells, especially those under hypoxic conditions.[40,41] The photoactivatable STING agonist **2** was designed containing the benzenesulfonamide moiety, a key pharmacophore that binds to CAIX. To determine whether **2** is accumulated in the tumor, flow cytometry assay was employed to measure the binding of the fluorescent **2** to the membrane CAIX of CT-26 colon cancer cells. As shown in Fig. 4A, a significant right shift of the fluorescence signal was observed for **2**, while there was no such shift for **1**. Accordingly, the mean fluorescence intensity of the wild type cells treated with **2** was significantly increased but not in the case of **1** (Fig. 4B). The fluorescence intensity in the CAIX-knocked down cells treated with **2** was decreased (Fig. 4C and

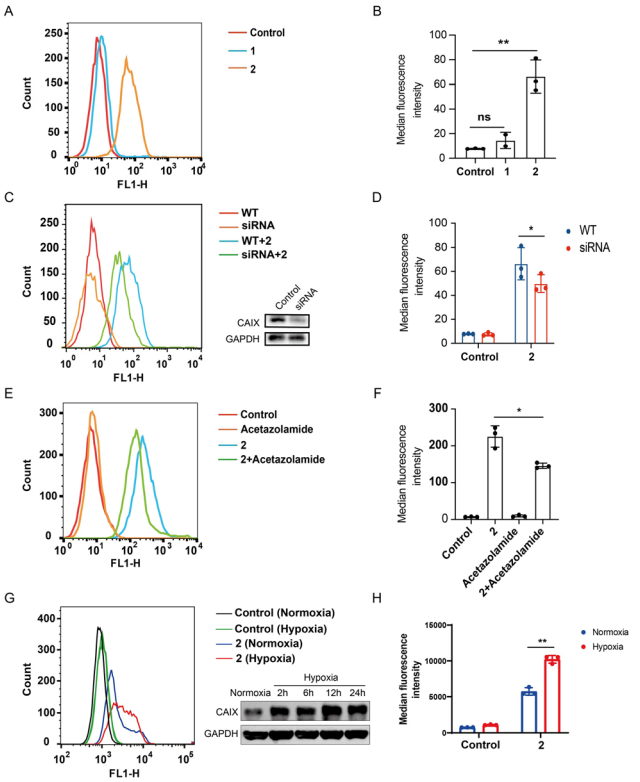


Fig. 4 Compound **2** binds to CAIX of CT26 colon cancer cells. (A) Flow cytometric analysis of CT-26 cells treated with **1** and **2** (10 μM), respectively; (B) median fluorescence intensity of (A); (C) flow cytometric analysis of wild type and CAIX knock-down CT-26 cells treated with **2** (10 μM) and western blotting analysis of the CAIX knock-down cells by siRNA; (D) median fluorescence intensity of (C); (E) flow cytometric analysis of CT26 cells treated with acetazolamide (10 μM) and **2** (10 μM), respectively, as well as the acetazolamide-preincubated CT26 cells treated with **2**; (F) median fluorescence intensity of (E). (G) CT26 cells were cultured under normoxia and hypoxia (0.5% $O_2$), and 24 h later the cells were incubated with or without **2** (10 μM) and subjected to flow cytometry analysis, besides the expression of CAIX was determined by western blotting at different time points; (H) median fluorescence intensity of (G). Results are expressed as mean ± SEM from two independent experiments (*$p$ < 0.05, **$p$ < 0.01, $t$-test).

D), suggesting CAIX is a target of **2** accounting for its specific targeting of CT-26 tumor cells. Moreover, pretreatment of CT-26 cells with acetazolamide,[42] a CAIX specific inhibitor, followed by **2** decreased the fluorescence intensity (Fig. 4E and F), compared to treatment with **2** alone, indicating acetazolamide competitively binding to CAIX with **2**. It seems that the binding of **2** to CAIX-expressing tumor cells is one of mechanisms for targeting tumor cells, while other pathways may exist, such as targeting other subtypes of carbonic anhydrase. Further, we compared the binding of **2** to CT26 cells under hypoxia and normoxia, and found that the binding was dramatically increased under hypoxia compared to normoxia, which was consistent with the increased expression of CAIX under hypoxia (Fig. 4G and H), indicating a binding advantage of **2** in the hypoxic tumor microenvironment. Similarly, the binding of **2** to HT29 colon tumor cells was dramatically increased under hypoxia compared to normoxia (Fig. S4A and B†), and also decreased by acetazolamide pre-treatment (Fig. S4C and D†). These results collectively illustrated that the photoactivatable agonist **2** possessed promising potential to accumulate in tumor tissues at least due to its CAIX binding capacity.

## Compound 2 photo-controllably activates STING signalling in zebrafish embryos and preferentially targets tumour cells in zebrafish xenografts

The zebrafish embryo model has various biological advantages, especially its *ex vivo* development and optical transparency, making it an ideal system for quickly monitoring drug responses *in vivo*.[43,44] The innate and adaptive immune systems in zebrafish are also highly conserved with mammals, and immune cells and cancer cells can be fluorescently labelled and directly observed in live zebrafish.[45,46] Thus, it is also frequently used to study the anti-tumor immune responses.[44,51]

We used the zebrafish containing fluorescent-labelled immune cells with Tg (*coro1a*:EGFP) or Tg (*mpeg1*:mCherry)

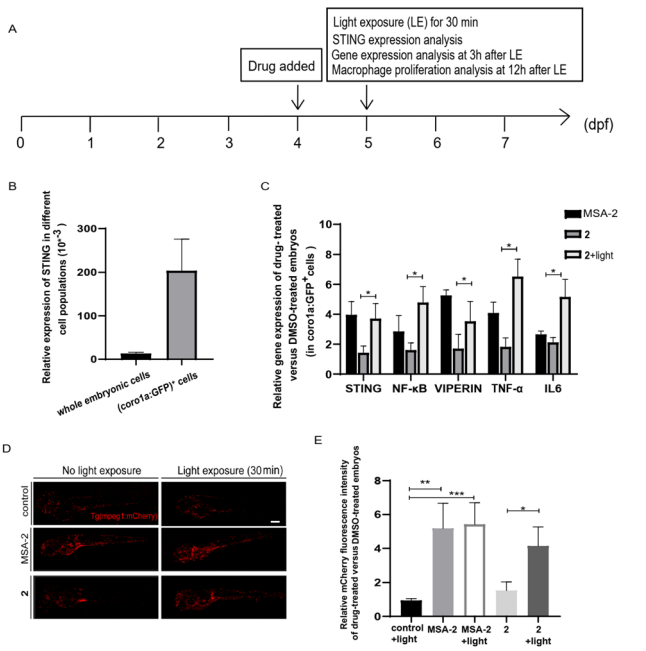


Fig. 5 Photo-triggered activation of the STING signalling pathway by **2** in zebrafish. (A) The time scheme for the experiments in (B)–(E). MSA-2 (40 μM) and **2** (10 μM) were added to the embryo medium accordingly. (B) STING is highly expressed in Tg (*coro1a*:EGFP)$^+$ cells (labelling macrophages and neutrophils). (C) Relative expression of the genes involved in the STING signalling activation in embryos after MSA-2 and **2** treatment with or without light irradiation compared to the DMSO-treated embryos in sorted *coro1a*:EGFP-labelled cells. Results are expressed as mean ± SEM from three independent experiments, $n$ = 50 embryos per condition (*$p$ < 0.05, $t$-test). (D) Representative confocal images of Tg (*mpeg1*:mCherry) embryos (mCherry fluorescence labelling macrophages) after DMSO, MSA-2 and **2** treatment with or without light irradiation. (E) Summary of relative mCherry fluorescent intensity from (D). Results are expressed as mean ± SEM from three independent experiments, $n$ = 15 embryos per condition (***$p$ < 0.001, **$p$ < 0.01, *$p$ < 0.05, $t$-test). Scale bar in (D): 125 μm; dpf, days post fertilization.

reporter as *in vivo* model organisms to evaluate photo-triggered activation of STING by **2**. Tg (*coro1a*:EGFP) labels macrophages and neutrophils in zebrafish embryos,[47] while Tg (*mpeg1*:mCherry) mainly marks macrophages.[48] As shown in Fig. 5A and B, STING is highly expressed in *coro1a*:EGFP$^+$ innate immune cells (macrophages and neutrophils). Photo-triggered STING activation assay was performed in the sorted *coro1a*:EGFP$^+$ cells. It has been reported that STING-dependent activation of IRF3 and NF-kB signalling varies between species.[49] Different from human and mouse STING alleles, activation of zebrafish STING (zSTING) causes dramatic enhancement of NF-kB signalling and weak IRF3-interferon signalling.[49] Therefore, the downstream NF-kB-related mRNA expression of zSTING was measured to monitor the light-induced activation of zSTING by **2**.[50] As shown in Fig. 5C, zebrafish at 4 days post-fertilization (dpf) was treated with **2** at 10 μM using MSA-2 (40 μM) as a positive control. After exposure to blue light at 450 nm for 30 min, zebrafish was incubated for another 3 h for mRNA expression analysis. As shown in Fig. 5C, zebrafish treated with **2** under blue light exposure significantly increased the mRNA expression of STING and its downstream NF-KB, VIPERIN, TNFA, and IL-6, a phenomenon similar to that of MSA-2. However, low expression of these effectors was observed for **2** without light irradiation, suggesting **2** could photo-controllably activate zSTING signalling in zebrafish embryo. In Tg (*mpeg1*:mCherry) zebrafish, the mCherry red fluorescence density is positively correlated with the number of macrophages. As illustrated in Fig. 5D and E, the vehicle group with light irradiation showed no significant difference in terms of fluorescence density relative to that without irradiation. The positive control group treated with MSA-2 significantly enhanced the fluorescence density regardless of light irradiation, indicating STING activation is beneficial for the proliferation of zebrafish macrophages. The zebrafish treated with **2** without irradiation displayed very weak red fluorescent intensity similar to that of the vehicle group. Upon 30 min light irradiation followed by incubation for another 12 h, the mCherry red fluorescence intensity was significantly enhanced to the level of the MSA-2 treated group, suggesting that decaging of **2** by blue light increased the number of macrophages in zebrafish. These results further confirmed that the light-induced activation of zSTING signalling by **2** could stimulate and activate innate immune cells in zebrafish embryo.

Moreover, zebrafish embryo xenografts of human cancer have been widely used to track tumor progression, drug responses, and tumor interaction with the host immune microenvironment due to the conserved cell intercommunication across species.[52–54] We then examined the targeting of compounds **1** and **2** to tumor cells in zebrafish xenografts. First, CT26 cells or HT29 human colon cells labelled with lipophilic dye DiI were microinjected into the yolk of 2 dpf zebrafish embryos to establish the xenograft model, by following the protocol as previously reported.[55,56] After incubation with **1** or **2** (10 μM) at 1 day-post-injection (dpi), as shown in the panel of merge in Fig. 6 and S5,† compound **2**, but not **1**, preferentially accumulated around HT29 or CT26 cells in injected embryos at 4 dpi, indicating tumor cell-targeting ability of **2** *in vivo*.

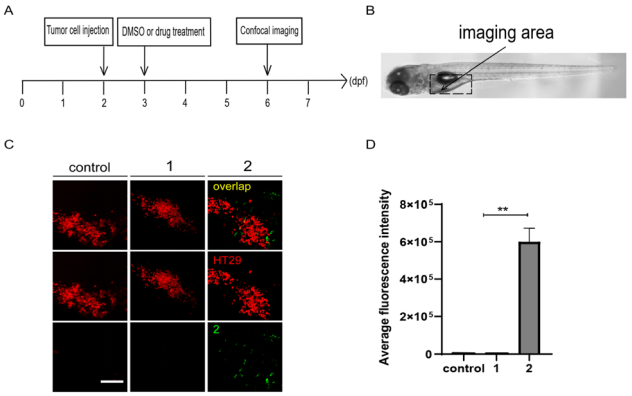


Fig. 6 Compound **2** targets tumor cells in zebrafish xenografts. (A) The time scheme for the experiments in (C) and (D). **1** (10 μM) and **2** (10 μM) were added to the embryo medium accordingly. (B) Scheme of the tumor cell injection site and subsequent imaging area. (C) Representative confocal images of HT29 tumor cells, compounds **1** and **2** in zebrafish xenografts at 6 dpf. (D) Summary of the fluorescent intensity of compounds **1** and **2** from (C), obtained by the excitation wavelength of 450 nm ($\lambda_{ex}$ = 450 nm). Results are expressed as mean ± SEM from three independent experiments, $n$ = 6–10 embryos per condition (**$p$ < 0.01, $t$-test). Scale bars in (C): 25 μm; dpf, days post fertilization.

## Photo-triggered activation of zSTING signalling by compound 2 stimulates immune cells to suppress tumor cell growth in zebrafish xenografts

We next investigated if photo-induced activation of zSTING signalling by **2** could activate immune cells to suppress tumor cell growth in zebrafish xenografts. To do that, we designed a dual-imaging assay (Fig. 7A and B). Briefly, Tg (*coro1a*:EGFP)-labelled zebrafish was implanted with CT26 or HT29 cancer cells at 2 dpf, and further incubated with **2** (10 μM) at 1 dpi using MSA-2 (40 μM) as the positive control. We confirmed that the fluorescence of **2** did not interfere with the fluorescence of Tg (*coro1a*:EGFP) (Fig. S6†). At 3 dpi, the zebrafish was irradiated by 450 nm blue light for 30 min. Confocal images were acquired at the tumor cell injecting area at 12 h after light exposure. As shown in Fig. 7C–F, the group treated with **2** in the absence of light irradiation exhibited similar fluorescence intensity of DiI to that of the control group, indicating no change of the tumor mass. Upon light irradiation, the Dil fluorescence intensity was significantly decreased, and the inhibitory rate was more than 50% compared with the control group, which is comparable to those of the MSA-2 group, suggesting potent photo-triggered inhibitory activity of **2** against CT26 or HT29 tumor growth.

We also compared the anti-tumoral effects of **1** and **2** in zebrafish larvae xenografted with HT29 cells. Without light activation, **1** and **2** showed minimal effects on tumor growth. After light activation, **2** showed a significantly increased inhibition of tumor growth compared with **1** (Fig. 8), supporting that enhanced tumor-targeting of **2** by CAIX increased anti-tumoral effects *in vivo*. Interestingly, both MSA-2 and **2** with or without light irradiation displayed no cytotoxic effects on

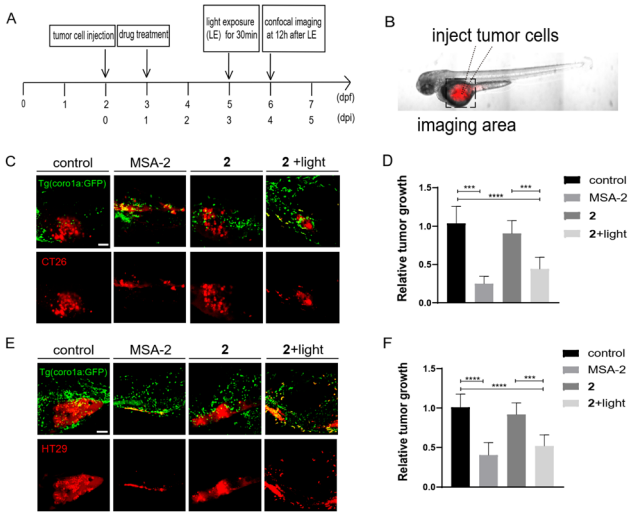


Fig. 7 Photo-triggered suppression of tumor cells by **2** in zebrafish xenografts. (A) The time scheme for the experiments in (C)–(F). MSA-2 (40 μM) and **2** (10 μM) were added to the embryo medium accordingly. (B) Scheme of the tumor cell injection site and subsequent imaging area. (C) Representative confocal images of CT26 tumor cells and innate immune cells from Tg (*coro1a*:GFP) zebrafish xenografts at 4 dpi treated with MSA-2, **2** and **2** irradiated by light. (D) Relative tumor growth at 4 dpi *versus* 1 dpi. Results are shown as the mean ± SEM from multiple experiments, $n = 9$ embryos per group (***$p < 0.001$, ****$p < 0.0001$, *t*-test). (E) Representative confocal images of HT29 tumor cells and innate immune cells from Tg (*coro1a*:GFP) zebrafish xenografts at 4 dpi treated with MSA-2, **2** and **2** irradiated by light. (F) Relative tumor growth at 4 dpi *versus* 1 dpi. Results are shown as the mean ± SEM from multiple experiments, $n = 9$ embryos per group (***$p < 0.001$, ****$p < 0.0001$, *t*-test). Scale bars in (C) and (E): 50 μm; dpf, days post fertilization; dpi, days post injection.

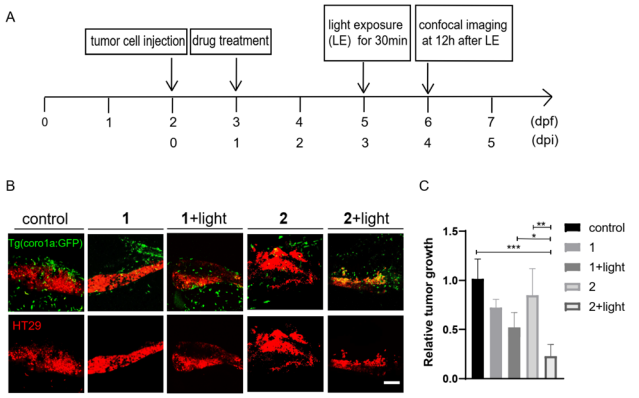


Fig. 8 Compound **2** displayed better antitumor effects than **1** in zebrafish xenografts. (A) The time scheme for the experiments in (B) and (C). **1** (10 μM) and **2** (10 μM) were added to the embryo medium accordingly. (B) Representative confocal images of HT29 tumor cells and innate immune cells from Tg (*coro1a*:GFP) zebrafish xenografts at 4 dpi treated with MSA-2, **1**, **2** or **1** and **2** irradiated by light. (C) Relative tumor growth at 4 dpi *versus* 1 dpi. Results are shown as the mean ± SEM from multiple experiments, $n = 6$–$9$ embryos per group (***$p < 0.001$, **$p < 0.01$, *$p < 0.05$, *t*-test). Scale bar: 25 μm; dpf, days post fertilization; dpi, days post injection.

CT26 and HT29 cells at various concentrations *in vitro* (Fig. S7†). Thus, the light-triggered anticancer activity of **2** is likely attributed to the STING-mediated activation of host immune cells, such as macrophages and neutrophils, to suppress tumor cell growth.

Indeed, as depicted in Fig. S8,† compared to the control or **2**-treated embryos without light irradiation, more Tg (*coro1a*:EGFP)-labelled immune cells were recruited to and co-localized with the CT26 or HT29 cells upon treatment with MSA-2 or **2** under light irradiation. Particularly, in the HT29 xenograft embryo, about 80% of tumor cells co-localized well with the immune cells after treatment with **2** irradiated by light or MSA-2, which is about 7-fold more than that without light exposure (Fig. S8C and D†). Besides, most of the immune cells have a rounded cellular morphology with fewer protrusions (Fig. S8C†), and they are likely phagocytotic macrophages exhibiting characteristics of killing tumor cells.[57,58] In contrast, more immune cells in the control or that without light irradiation remain separate from tumor cells that indicates their limited phagocytosis capability.[57,58] These results together suggested that photo-triggered activation of zSTING signalling by **2** stimulates host innate immune cells to suppress tumor cell growth in the zebrafish xenograft model.

Finally, we compared the toxicity of **2** and MSA-2 in live zebrafish with or without light irradiation. It was found that neither drug affected the overall survival of embryos, and **2** induced bent tails in about 25% of embryos after light activation, whereas MSA-2 caused bent tails in about 48% of embryos (Fig. S9†). In addition, **2** also induced significantly less cellular apoptosis-related gene expression compared with MSA-2 in the presence or absence of light (Fig. S9†). These results together support that the caged compound **2** has a better safety profile.

## Conclusions

Due to the potential "on-target off-tumor" toxicity arising from the ubiquitous activation of STING in various tissues in addition to tumor cells, clinical use of STING agonists is challenging. The controllable activation of the STING signalling specifically near cancerous tissues might be a promising option but with limited success yet. In this work, we designed and synthesized a three-component photo-caged STING agonist **2** by incorporating a photo-protecting group (DEACM), a tumor-targeting carbonic anhydrase IX warhead (arylsulfonamide), and a highly potent STING agonist (MSA-2). This caged STING agonist **2** could be readily uncaged by blue light irradiation to release the parent agonist MSA-2. In THP-1 cells, the caged agonist **2** without irradiation failed to stimulate STING activation; however, upon irradiation with biocompatible 450 nm blue light, it remarkably activated STING signalling leading to phosphorylation of its downstream proteins in a dose- and time-dependent manner. The tumor cell-preferring ability of **2** was further confirmed by flow cytometric analysis and fluorescence colocalization. More strikingly, photo-

triggered activation of STING signalling by **2** was demonstrated in the zebrafish embryo model, leading to upregulation of mRNA expression of the downstream NF-kB and cytokines and proliferation of zebrafish macrophages. Compared to **1** without the carbonic anhydrase warhead, compound **2** more preferentially targeted tumor cells in zebrafish xenografts, and photoactivation of **2** potently stimulated effector immune cells to display better antitumor effects than **1**, and lower systemic toxicity compared to MSA-2. Thus, compound **2** is a promising tumor cell-targeting photoactivatable STING agonist, which upon light irradiation, can efficiently release the "real" STING agonist and "turn on" the innate antitumor immunity.

The major conceptual advancement of this work is the achievement of the photo-controllable activation of STING signalling by a photo-caged CAIX-targeting STING agonist, thus exerting targeted anti-tumor effects in zebrafish xenografts. Since DEACM with 450 nm absorbance is used as PPG, our photo-caged STING agonist is limited by short irradiation light wavelength (<650 nm) for uncaging, which restricts the photo-release of STING agonists in deep tissues of mammalian animal models due to strong background light absorbance. Therefore, development of a photo-caged STING agonist with long wavelength of uncaging light (>650 nm) is highly desired for clinical translation. In the near future, we will develop new photo-removable protecting groups with long uncaging wavelength, instead of DEACM, to cage the STING agonist, and the related results will be reported in due course.

## Author contributions

C. D., Z. X., A. Z., and M. G. conceived and designed the project. M. D., Z. X., X. W., H. L., E. H., H. L., Y. D., Q. L., S. L., R. X., and X. W. performed the experiments. M. D., Z. X., X. W., E. H., H. L., Y. D., Q. L., R. X., Z. X., and X. W. collected and analyzed the data. C. D., Z. X., L. J., and A. Z. wrote the manuscript. C. D., L. J., Z. X., and A. Z. supervised the project. All authors discussed the results and commented on the manuscript.

## Conflicts of interest

There are no conflicts to declare.

## Acknowledgements

This work was sponsored by grants from the National Natural Science Foundation of China (21877120 and 22177068), Science and Technology Commission of Shanghai Municipality (21ZR1429100), Start-up grants from Shanghai Jiao Tong University (AF1700037 and WF220217002), Collaborative Innovation Cluster Project of Shanghai Municipal Commission of Health and Family Planning (2020CXJQ02), National Natural Science Foundation of China for Innovation Research Group (81821005) and the National Key R&D Program of China (2022YFF1203005).

## Notes and references

1 Q. Chen, L. Sun and Z. J. Chen, *Nat. Immunol.*, 2016, **17**, 1142.
2 M. H. Christensen and S. R. Paludan, *Cell. Mol. Immunol.*, 2017, **14**, 4.
3 C. Lu, J. Guan, S. Lu, Q. Jin, B. Rousseau, T. Lu, D. Stephens, H. Zhang, J. Zhu, M. Yang, Z. Ren, Y. Liang, Z. Liu, C. Han, L. Liu, X. Cao, A. Zhang, J. Qiao, K. Batten, M. Chen, D. H. Castrillon, T. Wang, B. Li, L. A. Diaz Jr, G.-M. Li and Y.-X. Fu, *Cancer Cell*, 2021, **39**, 96.
4 H. Ishikawa and G. Barber, *Nature*, 2008, **455**, 674.
5 H. Ishikawa, Z. Ma and G. N. Barber, *Nature*, 2009, **461**, 788.
6 D. L. Burdette, K. M. Monroe, K. Sotelo-Troha, J. S. Iwig, B. Eckert, M. Hyodo, Y. Hayakawa and R. E. Vance, *Nature*, 2011, **478**, 515.
7 W. Sun, Y. Li, L. Chen, H. Chen, F. You, X. Zhou, Y. Zhou, Z. Zhai, D. Chen and Z. Jiang, *Proc. Natl. Acad. Sci. U. S. A.*, 2009, **106**, 8653.
8 B. Zhong, Y. Yang, S. Li, Y.-Y. Wang, Y. Li, F. Diao, C. Lei, X. He, L. Zhang, P. Tien and H.-B. Shu, *Immunity*, 2008, **29**, 538.
9 X. Zhang, H. Shi, J. Wu, X. Zhang, L. Sun, C. Chen and Z. J. Chen, *Mol. Cell*, 2013, **51**, 226.
10 C. Zhang, G. Shang, X. Gui, X. Zhang, X.-C. Bai and Z. J. Chen, *Nature*, 2019, **567**, 394.
11 Y. Tanaka and Z. J. Chen, *Sci. Signaling*, 2012, **5**, ra20.
12 S. Liu, X. Cai, J. Wu, Q. Cong, X. Chen, T. Li, F. Du, J. Ren, Y.-T. Wu, N. V. Grishin and Z. J. Chen, *Science*, 2015, **347**, aaa2630.
13 L. Corrales, L. H. Glickman, S. M. McWhirter, D. B. Kanne, K. E. Sivick, G. E. Katibah, S.-R. Woo, E. Lemmens, T. Banda, J. J. Leong, K. Metchette, T. W. Dubensky Jr and T. F. Gajewski, *Cell Rep.*, 2015, **11**, 1018.
14 L. Corrales, S. M. McWhirter, T. W. Dubensky and T. F. Gajewski, *J. Clin. Invest.*, 2016, **126**, 2404.
15 G. Berger, M. Marloye and S. E. Lawler, *Trends Mol. Med.*, 2019, **25**, 412.
16 J. A. Trujillo, R. F. Sweis, R. Bao and J. J. Luke, *Cancer Immunol. Res.*, 2018, **6**, 990.
17 S.-R. Woo, M. B. Fuertes, L. Corrales, S. Spranger, M. J. Furdyna, M. Y. K. Leung, R. Duggan, Y. Wang, G. N. Barber, K. A. Fitzgerald, M.-L. Alegre and T. F. Gajewski, *Immunity*, 2014, **41**, 830.
18 S.-R. Woo, L. Corrales and T. F. Gajewski, *Annu. Rev. Immunol.*, 2015, **33**, 445.
19 H. Zhang, Q.-D. You and X.-L. Xu, *J. Med. Chem.*, 2020, **63**, 3785.
20 C. Ding, Z. Song, A. Shen, T. Chen and A. Zhang, *Acta Pharm. Sin. B*, 2020, **10**, 2272.
21 S. Vyskocil, D. Cardin, J. Ciavarri, J. Conlon, C. Cullis, D. England, R. Gershman, K. Gigstad, K. Gipson, A. Gould, P. Greenspan, R. Griffin, N. Gulavita, S. Harrison, Z. Hu, Y. Hu, A. Hata, J. Huang, S.-C. Huang, D. Janowick, M. Jones, V. Kolev, S. P. Langston, H. M. Lee, G. Li, D. Lok, L. Ma, D. Mai, J. Malley, A. Matsuda, H. Mizutani, M. Mizutani, N. Molchanova, E. Nunes, S. Pusalkar,

C. Renou, S. Rowland, Y. Sato, M. Shaw, L. Shen, Z. Shi, R. Skene, F. Soucy, S. Stroud, H. Xu, T. Xu, A. O. Abu-Yousif and J. Zhang, *J. Med. Chem.*, 2021, **64**, 6902.

22 F. Meric-Bernstam, S. K. Sandhu, O. Hamid, A. Spreafico and J. J. Luke, *J. Clin. Oncol.*, 2019, **37**(15 suppl.), 2507.

23 J. M. Ramanjulu, G. S. Pesiridis, J. Yang, N. Concha, R. Singhaus, S.-Y. Zhang, J.-L. Tran, P. Moore, S. Lehmann, H. C. Eberl, M. Muelbaier, J. L. Schneck, J. Clemens, M. Adam, J. Mehlmann, J. Romano, A. Morales, J. Kang, L. Leister, T. L. Graybill, A. K. Charnley, G. Ye, N. Nevins, K. Behnia, A. I. Wolf, V. Kasparcova, K. Nurse, L. Wang, A. C. Puhl, Y. Li, M. Klein, C. B. Hopson, J. Guss, M. Bantscheff, G. Bergamini, M. A. Reilly, Y. Lian, K. J. Duffy, J. Adams, K. P. Foley, P. J. Gough, R. W. Marquis, J. Smothers, A. Hoos and J. Bertin, *Nature*, 2018, **564**, 439.

24 Q. Xi, M. Wang, W. Jia, M. Yang, J. Hu, J. Jin, X. Chen, D. Yin and X. Wang, *J. Med. Chem.*, 2020, **63**, 260.

25 Z. Song, X. Wang, Y. Zhang, W. Gu, A. Shen, C. Ding, H. Li, R. Xiao, M. Geng, Z. Xie and A. Zhang, *J. Med. Chem.*, 2021, **64**, 1649.

26 B.-S. Pan, S. A. Perera, J. A. Piesvaux, J. P. Presland, G. K. Schroeder, J. N. Cumming, B. W. Trotter, M. D. Altman, A. V. Buevich, B. Cash, S. Cemerski, W. Chang, Y. Chen, P. J. Dandliker, G. Feng, A. Haidle, T. Henderson, J. Jewell, I. Kariv, I. Knemeyer, J. Kopinja, B. M. Lacey, J. Laskey, C. A. Lesburg, R. Liang, B. J. Long, M. Lu, Y. Ma, E. C. Minnihan, G. O'Donnell, R. Otte, L. Price, L. Rakhilina, B. Sauvagnat, S. Sharma, S. Tyagarajan, H. Woo, D. F. Wyss, S. Xu, D. J. Bennett and G. H. Addona, *Science*, 2020, **369**, eaba6098.

27 G. N. Barber, *Nat. Rev. Immunol.*, 2015, **15**, 760.

28 B. Larkin, V. Ilyukha, M. Sorokin, A. Buzdin, E. Vannier and A. Poltorak, *J. Immunol.*, 2017, **199**, 397.

29 J. Wu, Y.-J. Chen, N. Dobbs, T. Sakai, J. Liou, J. J. Miner and N. Yan, *J. Exp. Med.*, 2019, **216**, 867.

30 A. N. Ankenbruck, T. Courtney, Y. Naro and A. Deiters, *Angew. Chem., Int. Ed.*, 2018, **57**, 2768.

31 W. A. Velema, J. P. van der Berg, W. Szymanski, A. J. M. Driessen and B. L. Feringa, *ACS Chem. Biol.*, 2014, **9**, 1969.

32 M. Trebacz, Y. Wang, L. Makotta, L. Henschke and M. Köhn, *J. Org. Chem.*, 2020, **85**, 1712.

33 (*a*) J. Huey, K. Keutler and C. Schultz, *Cell Chem. Biol.*, 2020, **27**, 1015; (*b*) R. R. Nani, A. P. Gorka, T. Nagaya, T. Yamamoto, J. Ivanic, H. Kobayashi and M. J. Schnermann, *ACS Cent. Sci.*, 2017, **3**, 329.

34 S. Farley, A. Laguerre and C. Schultz, *Curr. Opin. Chem. Biol.*, 2021, **65**, 42.

35 (*a*) A. Bardhan and A. Deiters, *Curr. Opin. Struct. Biol.*, 2019, **57**, 164; (*b*) M. J. Hansen, F. M. Feringa, P. Kobauri and W. Szymanski, *J. Am. Chem. Soc.*, 2018, **140**, 13136.

36 A. Laguerre and C. Schultz, *Curr. Opin. Cell Biol.*, 2018, **53**, 97.

37 (*a*) M. J. Hansen, W. A. Velema, M. M. Lerch, W. Szymanski and B. L. Feringa, *Chem. Soc. Rev.*, 2015, **44**, 3358; (*b*) D. Liu, B. Yu, X. Guan, B. Song, H. Pan, R. Wang, X. Feng, L. Pan, H. Huang, Z. Wang, H. Wu, Z. Qiu, Z. Li and J. Bian, *Chem. Sci.*, 2023, **14**, 4174.

38 A. Laguerre, S. Hauke, J. Qiu, J. K. Martin and C. Schultz, *J. Am. Chem. Soc.*, 2019, **141**, 16544.

39 J. P. Olson, M. R. Banghart, B. L. Sabatini and G. C. R. Ellis-Davies, *J. Am. Chem. Soc.*, 2013, **135**, 15948.

40 Q. Cao, D.-J. Zhou, Z.-Y. Pan, G.-G. Yang, H. Zhan, L.-N. Ji and Z.-W. Mao, *Angew. Chem., Int. Ed.*, 2020, **59**, 18556.

41 N. Krall, F. Pretto, W. Decurtins, G. J. L. Bernardes, C. T. Supuran and D. Neri, *Angew. Chem., Int. Ed.*, 2014, **53**, 4231.

42 Z. Hou, B. Lin, Y. Bao, H.-N. Yan, M. Zhang, X.-W. Chang, X.-X. Zhang, Z.-J. Wang, G.-F. Wei, M.-S. Cheng, Y. Liu and C. Guo, *Eur. J. Med. Chem.*, 2017, **132**, 1.

43 D. J. Grunwald and J. S. Eisen, *Nat. Rev. Genet.*, 2002, **3**, 717.

44 G. Kari, U. Rodeck and A. P. Dicker, *Clin. Pharmacol. Ther.*, 2007, **82**, 70.

45 R. White, K. Rose and L. Zon, *Nat. Rev. Cancer*, 2013, **13**, 624.

46 M. Roh-Johnson, A. N. Shah, J. A. Stonick, K. R. Poudel, J. Kargl, G. H. Yang, J. d. Martino, R. E. Hernandez, C. E. Gast, L. R. Zarour, S. Antoku, A. M. Houghton, J. J. Bravo-Cordero, M. H. Wong, J. Condeelis and C. B. Moens, *Dev. Cell*, 2017, **43**, 549.

47 L. Li, B. Yan, Y. Q. Shi, W. Q. Zhang and Z. L. Wen, *J. Biol. Chem.*, 2012, **287**, 25353.

48 F. Ellett, L. Pase, J. W. Hayman, A. Andrianopoulos and G. J. Lieschke, *Blood*, 2011, **117**, e49.

49 C. C. de Oliveira Mann, M. H. Orzalli, D. S. King, J. C. Kagan, A. S. Y. Lee and P. J. Kranzusch, *Cell Rep.*, 2019, **27**, 1165.

50 R. Ge, Y. Zhou, R. Peng, R. Wang, M. Li, Y. Zhang, C. Zheng and C. Wang, *J. Virol.*, 2015, **89**, 7696.

51 N. S. Trede, D. M. Langenau, D. Traver, A. T. Look and L. I. Zon, *Immunity*, 2004, **20**, 367.

52 M. Hason and P. Bartůněk, *Genes*, 2019, **10**, 935.

53 V. Póvoa, C. Rebelo de Almeida, M. Maia-Gil, D. Sobral, M. Domingues, M. Martinez-Lopez, M. de Almeida Fuzeta, C. Silva, A. R. Grosso and R. Fior, *Nat. Commun.*, 2021, **12**, 1156.

54 X. Wang, W. Li, H. Jiang, C. Ma, M. Huang, X. Wei, W. Wang and L. Jing, *Int. J. Mol. Sci.*, 2022, **23**, 6442.

55 V. Póvoa, C. R. de Almeida, M. Maia-Gil, D. Sobral, M. Domingues, M. Martinez-Lopez, M. de Almeida Fuzeta, C. Silva, A. R. Grosso and R. Fior, *Nat. Commun.*, 2021, **12**, 1156.

56 C. J. Veinotte, G. Dellaire and J. N. Berman, *Dis. Models Mech.*, 2014, **7**, 745.

57 A. Fernandez, M. Vermeren, D. Humphries, R. Subiros-Funosas, N. Barth, L. Campana, A. MacKinnon, Y. Feng and M. Vendrell, *ACS Cent. Sci.*, 2017, **3**, 995.

58 C. Liu, C. Wu, Q. Yang, J. Gao, L. Li, D. Yang and L. Luo, *Immunity*, 2016, **44**, 1162.